Hindawi
Advances in Materials Science and Engineering
Volume 2021, Article ID 6466344, 9 pages
https://doi.org/10.1155/2021/6466344

Research Article

Study on the Optical Properties of High Refractive Index TeO_2-PbO-ZnO-BaF_2 Glass System

Shiyu Yin,[1] **Hao Wang**,[1] **Aifeng Li**,[2] **Haoyu Huang**,[3] **Jing Zhang**,[4] **Lin Liu**,[1] **and Yuanzhi Zhu**[1]

[1]*School of Mechanical and Materials Engineering, North China University of Technology, Beijing 100144, China*
[2]*College of Information Science and Engineering, Shandong Agricultural University, Taian 271018, China*
[3]*College of Architecture and Civil Engineering, Beijing University of Technology, Beijing 100124, China*
[4]*School of Information, North China University of Technology, Beijing 100144, China*

Correspondence should be addressed to Shiyu Yin; yinsy@ncut.edu.cn and Aifeng Li; liaf@sdau.edu.cn

Received 28 May 2021; Revised 26 August 2021; Accepted 4 September 2021; Published 21 September 2021

Academic Editor: Antonio Riveiro

The tellurite 60TeO_2-20PbO-(20-x)ZnO-xBaF_2 ($x = 1, 3, 5, 6, 7, 9$, and 11) series glass samples were prepared. The samples' SEM, XRD, DSC, density, refractive index, and absorption spectra were tested. A self-made optical platform was used to measure and calibrate the refractive index. The relationship between glass composition and crystallinity was discussed. The effects of density, molar refractive index, and metal standard value on the refractive index of glass samples were studied. The results showed that TPZBF glass has a high refractive index, and the refractive index increases with the increase in BaF_2 content.

1. Introduction

With the rapid development of precision optical instruments, optical information communication, optoelectronic products, and other fields, the demand for optical glass with excellent performance has increased, and the requirements are getting higher and higher. In optical design and communication, high-quality optical glass with a refractive index between 1.9 and 2.2 is significant to simplify the optical system and improve the imaging quality. It plays a vital role in the miniaturization of mobile phones, digital cameras, infrared applications, and the development of optical communication technology [1–3].

Tellurite glass uses TeO_2 as a leading glass-forming body. It has a higher refractive index ($n > 1.8$), a lower melting temperature (800–950°C), low phonon energy (600–850 cm^{-1}), good chemical stability, and other characteristics. It is an excellent material for preparing highly refractive index optical glass [4–6].

The TeO_2-PbO glass system has been extensively studied. This system has a large glass-forming area, good chemical stability, and thermal properties and is suitable for further research based on this system [7, 8]. Adding the transition metal zinc oxide to the glass system can extend the transparent area of the glass in the ultraviolet region. It can improve the moisture resistance, chemical durability, and thermal stability of the glass to a certain extent and comprehensively enhance the strength of the glass so that the glass can be a stable application under complicated working conditions [9–11]. Barium is the alkaline earth metal element with the most significant atomic number, largest ionic radius, and strongest basicity. Therefore, adding barium to the tellurite glass matrix adjusts the glass's structure and improves the glass's refractive index, density, gloss, and chemical stability. At the same time, a small amount of BaO will also accelerate the glass's melting and promote the glass's clarification [12, 13]. At present, studies have shown that TeO_2-PbO-ZnO system glass has excellent thermal stability, high mechanical strength, high absorption and emission cross section, broad effective fluorescence linewidth, long fluorescence lifetime, and low threshold. It is an ideal gain medium for realizing the high-energy ultrashort

tunable laser [14, 15]. In addition, there are studies on adding the TeO_2 to the B_2O_3-PbO-ZnO glass system to obtain boron tellurite glasses with high rare-earth ion doping concentrations. These glasses can be used in optical devices such as visible light lasers and fibre amplifiers. However, the composition of these glasses contains more B_2O_3, resulting in a lower refractive index of these glasses [9, 16]. Therefore, it is of great significance to study the factors affecting the refractive index of the TeO_2-PBO-ZnO-BaF_2 glass system for finding new optical materials.

The purpose of this research was to study the TeO_2-PbO-ZnO-BaF_2 glass system by measuring its scanning electron microscopy (SEM), X-ray diffraction (XRD), differential scanning calorimetry (DSC), density, refractive index, absorption spectrum, and so on. The relationship between refractive index and glass composition is discussed.

2. Materials and Methods

2.1. Fabrication of Glass. The conventional melt quenching technique was adopted to synthesise 60TeO2-20PbO-(20-x) ZnO-xBaF2 (where $x = 1$, 3, 5, 6, 7, 9, and 11 mol %) glasses, named TPZBF−1,−3, −5, −6, −7, −9, and −11, respectively. We used reagent-grade chemicals as raw materials and mixed them evenly after weighing. Each batch was melted in a pure Al_2O_3 ceramic crucible in the range of 850°C for 1.5 h and then cast onto the 200–250°C preheated brass mould. The obtained bulk glass was annealed and cooled to room temperature from 250°C to 300°C at a cooling rate of 1°C/min. The cooled glass was cut into glass pieces of about $20 \times 10 \times 1$ mm, and the surfaces of 20×10 mm and 20×1 mm were optically polished.

2.2. Refractive Index Test of Glass. The refractive index was measured using a self-made optical platform. The structure diagram of the platform is shown in Figure 1. The light source was provided by a He-Ne laser (LSR650NL-100) with a wavelength of 650 nm. The beam emitted from the laser was linearly polarised light with a diameter of about 3 mm. The beam was thicker and had low intensity; therefore, two convex optical lenses were used to focus the beam. As shown in Figure 1, the second convex lens located was twice the focal length of the first convex lens. A high-intensity parallel beam with a diameter of about 0.8 mm was obtained through the convex lens's focusing effect. The end of the optical platform had a unique inclination angle, where it could install adjustment blocks of different angles (30°, 45°, and 60°). We used screws to fix the angle adjustment block and platform together and then inserted baffles into the groove of the platform. On the one hand, the baffle could firmly lock the angle adjustment block and the convex lens on the platform, and on the other hand, it could help locate the angle and reduce the error in the measurement.

The position of the light beam passing through the glass was recorded on a unique piece of paper. We marked the paper with the tangent, normal, and positioning lines on the stage. The paper sheet is shown in Figure 2(a). The positioning lines on the paper sheet coincided with the edge of the stage. In addition, the height of the stage could be adjusted. Then, the glass was placed on the stage, the edge of the 20×1 mm surface of the glass was bonded to the tangent line, and the glass and the stage were glued together. After that the stage was pressed onto the angle adjustment block's oblique side to find a convenient position for observation and recording, as shown in Figure 2(b). We beamed the light across the glass at the intersection of the tangent line and normal line on the paper sheet, fixed the stage firmly on the base, adjusted it to the appropriate height, and started the test.

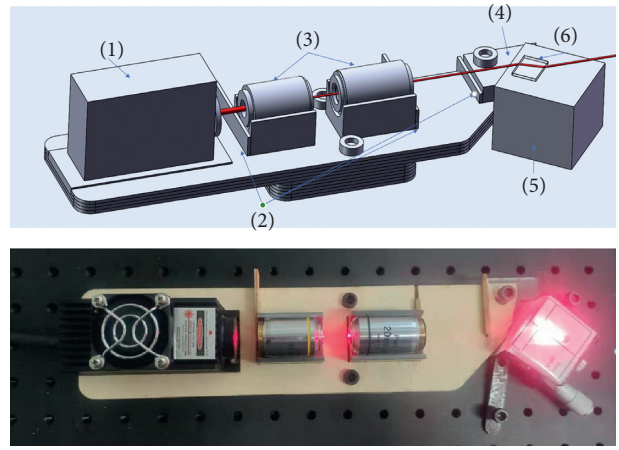

Figure 1: Schematic and actual setup for the refractive index test platform. 1: He-Ne laser, 2: baffles, 3: optical convex lens, 4: angle adjustment block, 5: height-adjustable stage, and 6: glass sample.

It should be noted that after starting the test, except for the replacement of the paper sheet and angle adjustment block, other parts of the platform were not disassembled to avoid other errors.

After starting the test, we could observe the light passing through the glass and refracting, as shown in Figure 2(c). We marked the position where the light exited from the glass with a needle and pierced a spot as small as possible on the paper. After the test, we scanned the paper with a printer and uploaded it to the computer to accurately measure the refraction angle. We used computer aided design software to open the scanned picture, connected the incident point and the exit point, and measured the angle between the normal line and this line. This angle is the angle of refraction, as shown in Figure 2(d). We measured six data at each grade (30°, 45°, and 60°), found the average value, and put it into the following formula:

$$n = \frac{\sin \alpha}{\sin \beta}, \tag{1}$$

where n is the refractive index, α is the angle of incidence, and β is the angle of refraction.

In the case of incident angles of 30°, 45°, and 60°, test the samples to find the average refraction angle at each incident angle and put the average refraction angle into equation (1) to find the corresponding refraction rate. Then, take the average of the three refractive indexes measured at the incident angle of 30°, 45°, and 60°, and the average value

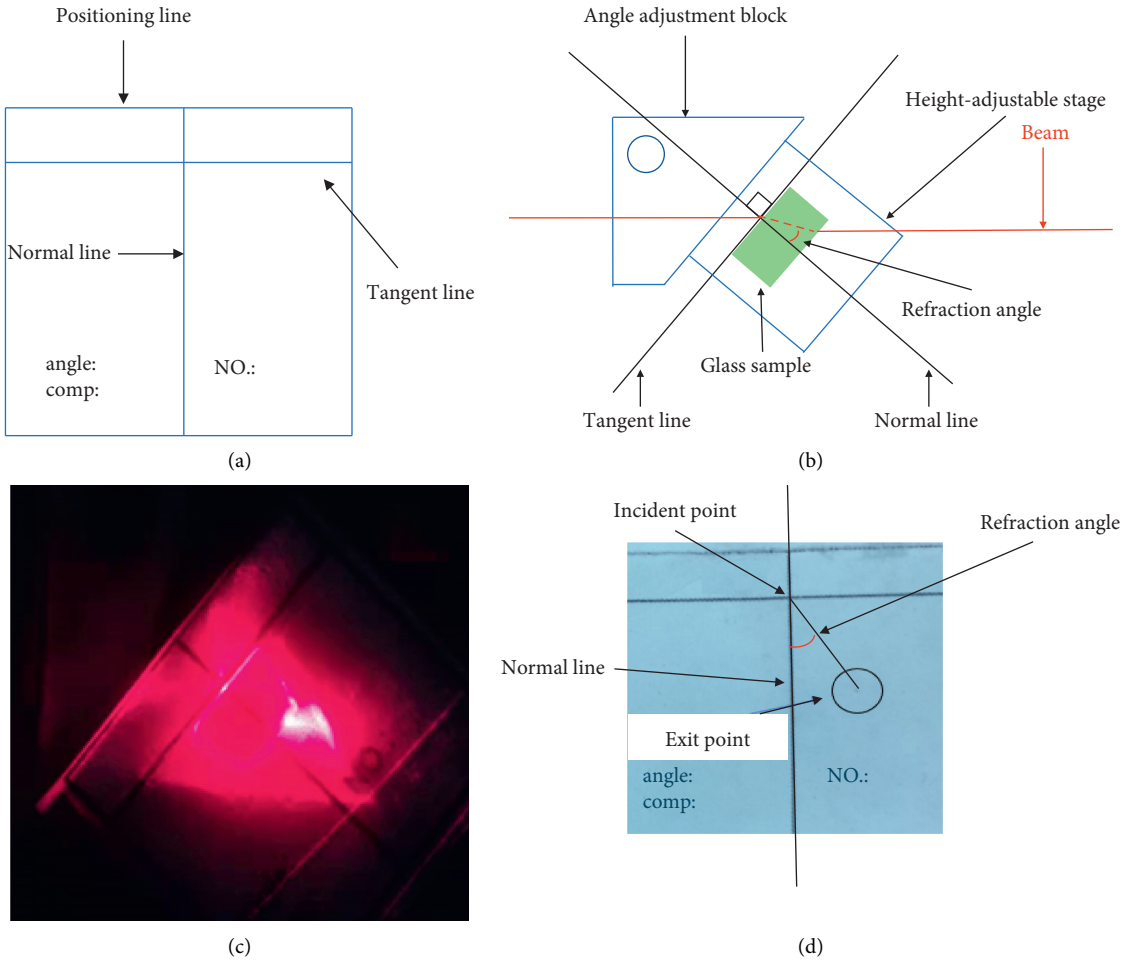

FIGURE 2: (a) Paper with positioning lines. (b) Schematic diagram of measurement. (c) Physical image of measurement. (d) Use computer aided design software to measure refraction angle.

obtained is the measured refractive index n_{test} obtained by the optical platform.

To eliminate error, the following formula was used to correct the measured refractive index n_{test}:

$$n_{theory} = a \times n_{test} + b, \quad (2)$$

where n_{theory} is the theoretical refractive index and a and b are two correction coefficients. To obtain a and b, the standard optical quartz glass and an ellipsometer were used for calibration.

The refractive index of the standard optical quartz glass under the irradiation of visible light with a wavelength of 650 nm was 1.4565. The self-made optical platform was used to test the standard optical quartz glass under the same conditions, taking its test and theoretical values as conditions for finding a and b. Then, the refractive index of TPBZF-1 glass was measured with an ellipsometer (J. A. Woollam Co., Inc. M2000XF), and the theoretical and measured values of TPBZF-1 glass were used as the other conditions for finding a and b. Bringing these two conditions into equation (2), getting the values of a and b, and then bringing the measured values of other glasses into equation (2) got the corresponding modified glass refractive index n.

2.3. Other Characterisations of the Glass. The prepared glasses were subjected to different characterisations: SEM was performed using a high-resolution environmental scanning electron microscope (FEI Quanta 650). SEM images were obtained in a high vacuum mode and with an acceleration of 500 kV. To eliminate the charging effect, the sample surface was sprayed with gold; X-ray diffraction (Ultima IV) patterns were determined at room temperature with a diffraction angle of $2\theta = 10^{\circ}$–100° and at a rate of 0.02°/min; glass transition temperature and crystallisation temperature were determined by DSC (NETZSCH STA 449F3). A 10 mg sample was heated in Al_2O_3 crucible at a heating rate of 30°C/min in N_2 gas atmosphere; the density was measured according to the Archimedes principle using pure water ($\rho = 0.99980$ g/cm^3, 16°C) as immersion liquid at room

temperature; the absorption spectra were measured in the wavelength range of 190 nm to 900 nm using a UV-VIS spectrophotometer (PerkinElmer Lambda 650) with optically polished samples of approximately 5 mm thickness.

3. Results and Discussion

3.1. Scanning Electron Microscope (SEM). The fabricated TPZBF1-7 glass was clear, bright, and light green glass. TPZBF-9 glass was also relatively clear but had obvious crystallisation points. TPZBF-11 glass was completely crystallised and could not transmit light.

SEM images for the TPZBF-7 glasses are presented in Figure 3(a). These images show a glassy surface with no crystal precipitate since only the common constituents were present. TPZBF1-7 sample profiles were found to be similar. The TPZBF-9 sample had obvious crystallisation points on the surface; the SEM image of the crystallisation point position is shown in Figure 3(b).

3.2. X-Ray Diffraction (XRD). The XRD diffraction pattern of TPZBF glass is shown in Figure 4. It can be seen from Figure 4 that when $x = 0$ and 7, the X-ray pattern of the glass powder is basically the same. They have a wide diffraction peak near $2\theta = 30^\circ$ and $2\theta = 50^\circ$, respectively, in the diffraction pattern. There is no very sharp diffraction peak, which is a very typical diffraction pattern of an amorphous substance. These show that when the mole percentage of BaF_2 is between 1% and 7% (corresponding to the mole percentage of ZnO between 19% and 13%), the product obtained after the smelting of the TPZBF glass system is a stable glass structure without precipitation of crystalline phases [17].

In the glass melting process, a part of BaF_2 combines with O_2 in the environment and is transformed into BaO that enters the glass network as a modifier and F_2 that escapes to the atmosphere; the other part of BaF_2 breaks the MO bond (M = Te, Pb, Zn) and enters the glass network to form an oxyfluoride glass structure. Hence, the crystallisation tendency of the glass increases sharply and crystalline phases begin to appear. When the mole percentage of BaF_2 reaches 11%, the glass is completely crystallised. The crystalline phases observed in the TPZBF-9 sample were identified as PbF_2 and Ba_2ZnF_6. We found that a chemical reaction occurs in the melt that forms the glass, the content of which is as follows:

$$PbO + ZnO + BaF_2 \longrightarrow PbF_2 + Ba_2ZnF_6 + O_2\uparrow. \quad (3)$$

The addition of excess F element replaces the O element in the glass network structure, leading to these PbF_2 and Ba_2ZnF_6 crystalline phases. In Figure 4, the phase peaks of the PbF_2 crystal are located at $2\theta = 28.9^\circ$, 42.7°, 47.0°, and 48.2°, respectively, while the phase peaks of the Ba_2ZnF_6 crystal are located at $2\theta = 39.2^\circ$.

3.3. Differential Scanning Calorimetry (DSC). Figure 5 is the DSC spectrum of TPZBF-7 glass. From the figure, the glass transition temperature T_g, the onset of crystallisation temperature T_c, and the difference ΔT of the glass can be estimated. The values of T_g, T_c, and ΔT are 266, 325, and 59°C, respectively.

The ΔT value can be used to evaluate the thermal stability of the glass. The larger the ΔT, the wider the operable range without devitrification during glass melting and the better the thermal stability. The ΔT value of the TPZBF-7 sample is 59°C, which is a small value in tellurite glass. It can also be seen from Figure 5 that the first crystallisation peak of the glass is next to the glass transition temperature peak, so the series of glasses are relatively easy to crystallize [18–20].

3.4. Density. The composition and density of the glass are shown in Table 1. As the TPZBF-11 component glass was devitrified, the properties of TPZBF-11 are not studied below. It can be seen from Table 1 that as BaF_2 gradually replaced ZnO, the density of the glass gradually increased from 6.243 g/cm^3 to 6.327 g/cm^3.

The density of the glass depends not only on the mass of the atoms constituting the glass but also on the tightness of the atomic packing and the coordination number. The following two aspects mainly determine the gradual increase in density of TPZBF series glass. On the one hand, the relative atomic mass of Ba is 137.32, while the relative atomic mass of Zn is 65.38, which is much lower than Ba. On the other hand, according to the classification of oxides in the glass network, BaO and ZnO belong to modified bodies and intermediates, respectively. As a modified body, BaO can enter the structural gaps of the glass network, making the structure of the glass more compact, thereby increasing the density. Since the polarisability of Zn^{2+} ions is lower than that of Ba^{2+} and Pb^{2+} ions, ZnO tends to play the role of network structure in the glass network (for example, in the TeO_2-ZnF_2-ZnO glass system, Zn^{2+} participates in the formation of the glass network in the form of zinc oxide tetrahedrons [21]). The decrease in ZnO weakens the construction of the glass network, which reduces the molecular volume and increases the glass density. Therefore, under the combined effect of the above two reasons, when BaF_2 replaces ZnO, the density of the glass increases significantly.

In addition, although the density of the glass increases, the increase is not apparent. This is because the glass composition contains 20% PbO (molar ratio). PbO is also a glass network modification body, and the molecular weight of Pb is greater than that of Ba, so the addition of BaF_2 can only slightly increase the density of the glass.

3.5. Refractive Index and Factors Affecting the Refractive Index. The refractive index n_{theory} of TPZBF-1 glass and standard optical quartz glass was measured with an ellipsometer. The test refractive index n_{test} of TPZBF1-9 glass was measured with a self-made optical platform. The n_{theory} and n_{test} of the two were brought into equation (2) and calculated as a and b:

$$a = \frac{n_{\text{theory·Quartz}} - n_{\text{theory·TPZBF-1}}}{n_{\text{test·Quartz}} - n_{\text{test·TPZBF-1}}},$$
$$b = n_{\text{theory·TPZBF-1}} - a \times n_{\text{test·TPZBF-1}}. \quad (4)$$

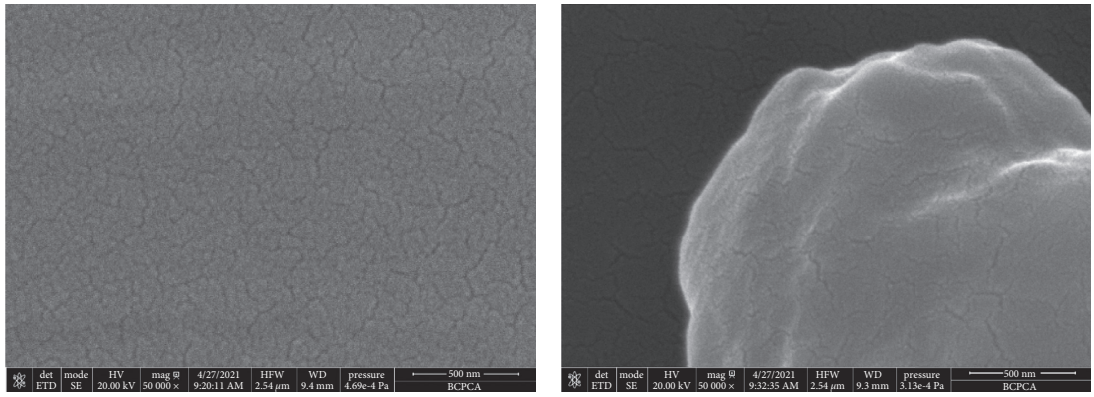

(a) (b)

Figure 3: SEM micrographs of TPZBF7 (a) and TPZBF9 (b).

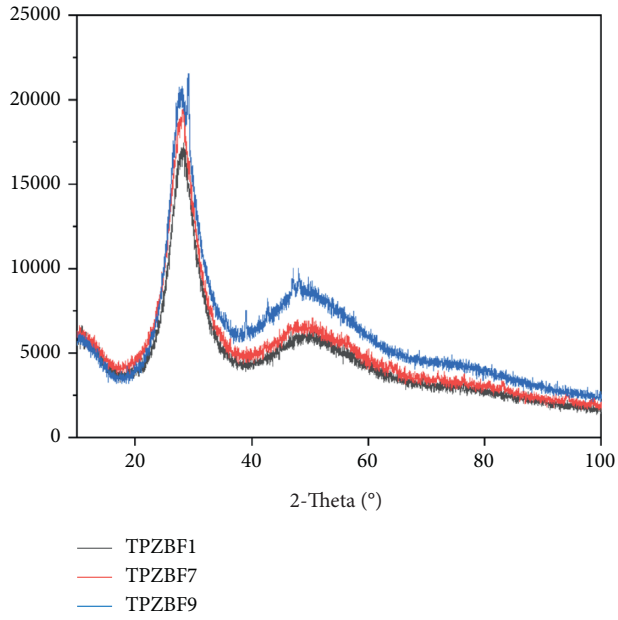

Figure 4: X-ray diffraction pattern of samples TPZBF-1, TPZBF-7, and TPZBF-9.

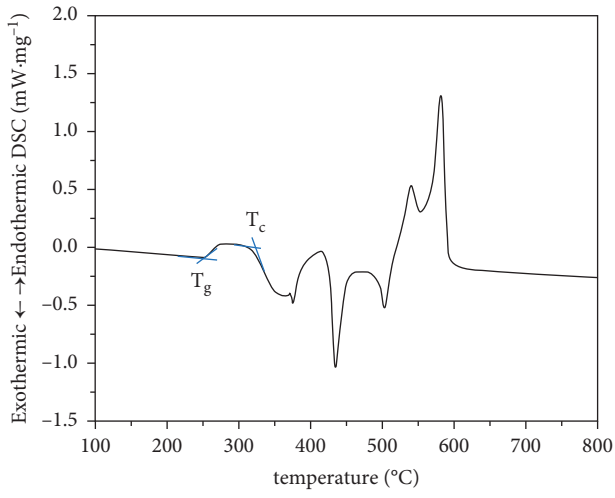

Figure 5: Differential scanning calorimetry of sample TPZBF-7.

Table 1: Compositions and density of glass sample.

Sample	Mole fraction (%)				Density d (g·cm^{-3})
	TeO_2	PbO	ZnO	BaF_2	
TPZBF1	60	20	19	1	6.243
TPZBF3	60	20	17	3	6.267
TPZBF5	60	20	15	5	6.295
TPZBF6	60	20	14	6	6.306
TPZBF7	60	20	13	7	6.313
TPZBF9	60	20	11	9	6.327

The value of a is 0.9821, and the value of b is 0.0246. The n_{test} of TPZBF1-9 glass was then brought into equation (2) to obtain the correct refractive index n of each component glass. The results are shown in Table 2.

$$n_{\text{TPZBF}-i} = a \times n_{\text{test·TPZBF}-1} + b. \tag{5}$$

The self-made optical platform had a refractive index error of 0.0824% for the standard optical quartz glass and 0.5521% for glass with a composition of TPZBF-1. The values of these two errors were below 1%. Therefore, the measurement result is relatively accurate.

The refractive index and other physical properties of the glass are shown in Table 3.

It can be seen from Table 3 that as BaF_2 replaced ZnO, the refractive index of the glass increased. The refractive index of glass depends on the density of the glass and the polarisability of internal ions.

H. N. Ritland's research shows that the refractive index of glass is a single-valued function of the density [22]. Generally, the greater the density of the glass, the denser the glass network and the more compact the structure and the slower the propagation of light in the glass, so the refractive index increases accordingly. Conversely, the lower the density, the smaller the refractive index. The density and refractive index of TPZBF series glass also conform to this rule.

According to Maxwell's electromagnetic field theory, the propagation speed of light in a medium should be

$$v = \frac{1}{\sqrt{\varepsilon\mu}} = \frac{1}{\sqrt{\varepsilon_0\mu_0}} \times \frac{1}{\sqrt{\varepsilon_r\mu_r}} = \frac{c}{\sqrt{\varepsilon_r\mu_r}} = \frac{c}{n}. \tag{6}$$

The expression of n is inferred from the following:

$$n = \sqrt{\varepsilon_r\mu_r}, \tag{7}$$

where c is the speed of light in a vacuum, μ is the magnetic permeability of the medium, ε is the dielectric constant of the medium, μ_0 is the magnetic permeability in a vacuum, ε_0 is the dielectric constant in a vacuum, μ_r is the relative permeability of the medium, and ε_r is the relative dielectric of the medium electric constant. In dielectrics such as inorganic materials, $\mu_r \approx 1$, so $n \approx \varepsilon_r^{1/2.}$

This shows that the refractive index of the medium increases with the increase in its dielectric constant. The dielectric constant is related to the polarisation of the medium. The higher the polarisation of the medium, the greater the refractive index.

Table 2: n_{theory}, n_{test}, and n of each component glass, at 650 nm.

	n_{theory}	n_{test}	N	Error (%)
Quartz glass	1.4565	1.4553	1.4565	0.0824
TPZBF1	2.0106	1.9995	2.0106	0.5521
TPZBF3		2.0437	2.0320	
TPZBF5		2.0644	2.0523	
TPZBF6		2.0814	2.0690	
TPZBF7		2.0891	2.0766	
TPZBF9		2.1102	2.0973	
TPZBF11		Crystallization		

When light passes through the glass, it causes the polarisation of the ions inside the glass. The polarisation of the ions, in turn, affects the propagation speed of the light wave in the glass. The greater the polarisability, the greater the energy absorbed after the light wave passes, the more significant the reduction in propagation speed, and the greater the refractive index.

The polarisation process is divided into passive polarisation and active polarisation [23]. Passive polarisation means that an ion is polarised under an external electric field generated by other ions. The polarisation rate α expresses its magnitude. Active polarisation means that an ion uses its electric field to act on surrounding ions to polarise other ions. Generally, the anion (O^{2-}, F^-) has a large radius and is easy to deform and polarise but the active polarisation ability is low. The cation radius (Te^{4+}, Pb^{2+}, Ba^{2+}, and Zn^{2+}) is relatively small, and when the electricity price is high, its active polarisation effect is large but the polarisation degree is low. The radius and polarisability of the ions contained in the TPZBF series glass are shown in Table 4.

The polarisability of Ba^{2+} ions is much higher than that of Zn^{2+} ions, so as BaF_2 replaces ZnO, the refractive index of the glass increases.

It can be seen from Table 4 that the ionic radius of Ba^{2+} ions was also larger than that of Zn^{2+} ions. When the radius of cations with the same atomic valence increased ($Ba^{2+} \longrightarrow Zn^{2+}$), the molar volume and molar refraction of the glass increased at the same time, and the increase in the molar volume reduced the refraction of the glass. The increase in the molar refraction increased the refractive index of the glass, so there was no linear relationship between the refractive index of the glass and the ionic radius. However, it can be demonstrated from other angles that the large ion radius of Ba^{2+} ions can provide glass with a higher refractive index.

The molar volume R_m of the glass can be calculated using the following formula [24]:

$$R_m = \frac{\left(n^2 - 1\right)}{\left(n^2 + 1\right)}\left(\frac{M}{d}\right), \tag{8}$$

where M is the molar mass of the glass, d is the density, and n is the refractive index of the glass.

The refractive index of glass can be regarded as the sum of its linear and nonlinear refractive indexes, as shown in the following formula [25]:

Table 3: Physical parameters of TPZBF glasses.

Sample	Molar mass M (g·mol^{-1})	Molar volume V_m (cm^3·mol^{-1})	Molar refraction R_m (cm^3·mol^{-1})	R_m/V_m	Refractive index n
TPZBF1	157.6150	25.2467	15.2331	0.6033	2.0106
TPZBF3	159.4942	25.4599	15.5261	0.6100	2.0320
TPZBF5	161.3734	25.6351	15.7984	0.6162	2.0523
TPZBF6	162.3130	25.7395	15.9914	0.6212	2.0690
TPZBF7	163.2526	25.8598	16.1239	0.6235	2.0766
TPZBF9	165.1318	26.0995	16.4309	0.6295	2.0973

Table 4: Ion radius and polarisability [23].

Ion	Te^{4+}	Pb^{2+}	Ba^{2+}	Zn^{2+}	O^{2-}	F^-
Ion radius/nm	0.056	0.120	0.135	0.074	0.140	0.136
Polarizability/$\times 10^{-3}$ nm^3	0.750	2.000	1.550	0.288	3.880	1.040

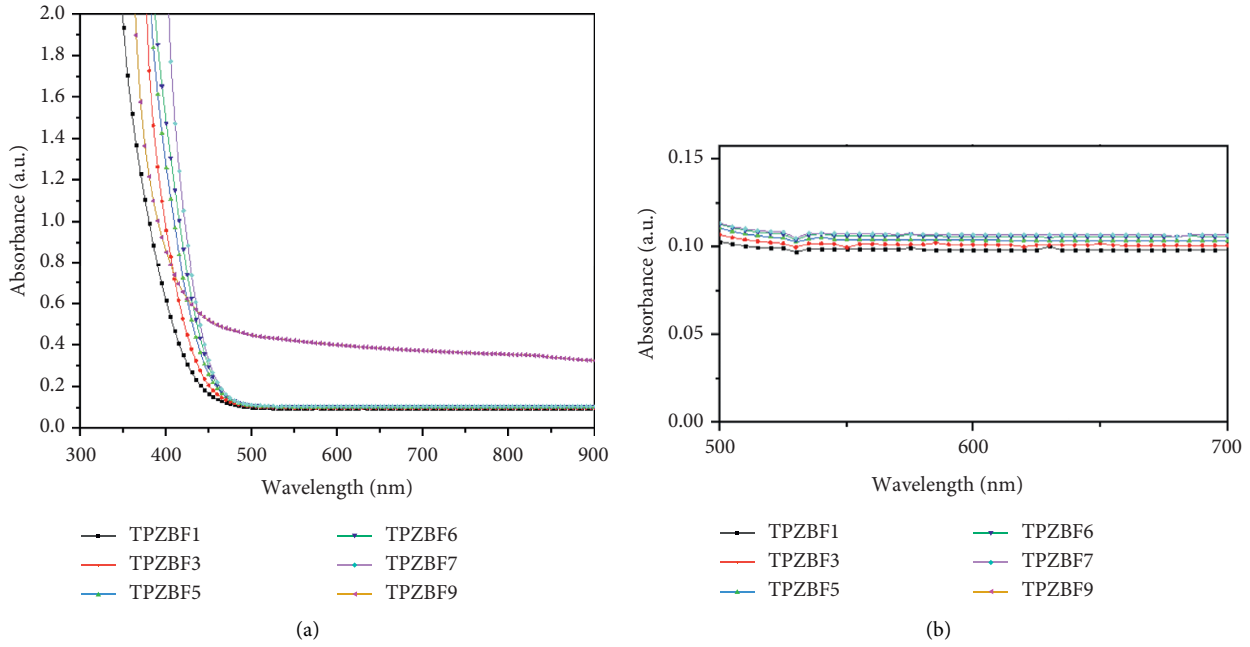

Figure 6: Optical absorbance spectra of TPZNF glasses in the 300–900 nm range (a) and in the 500–700 nm range (b).

$$n = n_0 + n_0 E^2, \tag{9}$$

where n_0 is the linear refractive index, n_2 is the nonlinear refractive index, and E is the field strength of the beam. This means that the higher the nonlinear refractive index n_2, the higher the refractive index n of the glass.

According to the research conclusion of Nasu [26], the nonlinear refractive index n_2 of glass is directly proportional to the ratio of molar refractive index to molar volume (R_m/V_m). The molar volume V_m, molar refractive index R_m, and their ratio of the glass are shown in Table 3. As the content of BaF_2 increased, the value of R_m/V_m of the glass increased from 0.6033 to 0.6295. Therefore, the replacement of ZnO by BaF_2 increased the refractive index of the glass.

3.6. Absorption Spectrum. Figure 6 shows the absorption spectra of the TPZBF glasses. It can be seen from the figure that as BaF_2 gradually replaced ZnO, the absorption boundary of the glass in the ultraviolet region gradually shifted to the long-wavelength direction. This phenomenon is mainly because the polarisability of Ba^{2+} ions is higher than that of Zn^{2+}, which leads to stronger absorption of ultraviolet light by the glass, which shifts the absorption boundary to the long-wavelength direction.

The TPZBF-9 sample underwent a certain degree of crystallisation, so its transmittance was also affected accordingly and was significantly lower than that of other glasses in the system.

The small picture on the upper righthand corner of Figure 6 is a partial picture of the 500–700 nm segment. It can be seen from the picture that as BaF_2 gradually replaced ZnO, the absorption strength of the glass decreased. This is because the following formula exists in the transparent area of the glass [27]:

$$\mathrm{OD} = \lg\left(\frac{n^2+1}{2n}\right), \tag{10}$$

where OD is the optical density and n is the refractive index of glass. If OD is regarded as a function of n, when $n > 1$, OD monotonically decreases, that is to say, the higher the refractive index, the lower the absorption intensity. The absorption intensity of TPZBF series glass in this area decreases with the increase of BaF2 content. This phenomenon is consistent with the change rule of refractive index.

4. Conclusions

$60TeO_2$-20PbO-(20-x)ZnO-xBaF_2 tellurite series glass was prepared, and SEM, XRD, DSC, density, refractive index, and absorption spectrum tests were carried out. A refractive index test platform for bulk solids was established, and the error was found to be within 1% after testing with standard optical quartz glass and TPZBF series glass.

Through the test and calculation of the prepared TPZBF series glass, the following regular was found. As the BaF_2 in the glass composition replaces ZnO, the density and refractive index of the glass gradually increase. The absorption edge in the absorption spectrum shifts to the long-wavelength direction, and the ultraviolet absorption increases. When the molar ratio of the BaF_2 component exceeds 9%, the glass begins to show a more obvious tendency to crystallize and the transmittance is significantly reduced.

Data Availability

The data in the article are available if necessary.

Conflicts of Interest

The authors declare that they have no conflicts of interest.

Acknowledgments

This work was funded by Scientific Research Project of Beijing Educational Committee (110052971803/069); Natural Sciences Foundation of China (11963004); and Shandong Province Natural Science Foundation (ZR2020MA095).

References

[1] T. Kim, M. Z. Bin Mohd Zawawi, R. Shin et al., "Replication of high refractive index glass microlens array by imprinting in conjunction with laser assisted rapid surface heating for high resolution confocal microscopy imaging," *Optics Express*, vol. 27, no. 13, pp. 18869–18882, 2019.

[2] D. Ramachari, C.-S. Yang, O. Wada, T. Uchino, and C.-L. Pan, "High-refractive index, low-loss oxyfluorosilicate glasses for sub-THz and millimeter wave applications," *Journal of Applied Physics*, vol. 125, no. 15, Article ID 151609, 2019.

[3] T. Toney Fernandez, P. Haro-González, B. Sotillo et al., "Ion migration assisted inscription of high refractive index contrast waveguides by femtosecond laser pulses in phosphate glass," *Optics Letters*, vol. 38, no. 24, pp. 5248–5251, 2013.

[4] Y. Al-Hadeethi and M. I. Sayyed, "The influence of PbO on the radiation attenuation features of tellurite glass," *Ceramics International*, vol. 45, no. 18, pp. 24230–24235, 2019.

[5] G. Kilic, E. Ilik, S. A. M. Issa, and H. O. Tekin, "Synthesis and structural, optical, physical properties of Gadolinium (III) oxide reinforced TeO2-B2O3-(20-x)Li2O-xGd2O3 glass system," *Journal of Alloys and Compounds*, vol. 877, no. 5, Article ID 160302, 2021.

[6] Y. Al-Hadeethi and M. I. Sayyed, "Radiation attenuation properties of Bi2O3-Na2O- V2O5- TiO2-TeO2 glass system using Phy-X/PSD software," *Ceramics International*, vol. 46, no. 4, pp. 4795–4800, 2020.

[7] S. H. Alazoumi, H. A. A. Sidek, R. El-Mallawany, H. M. Kamari, M. H. M. Zaid, and E. A. G. E. Ali, "Elastic moduli of TeO2-PbO glass system," *Applied Physics A*, vol. 124, no. 12, 845 pages, 2018.

[8] Y. Li, Q. Zhang, J. Song, X. Gao, W. Tang, and A. Lu, "Glass formation and spectral studies of PbO and Bi 2 O 3 modified TeO 2 -ZnO glasses," *Journal of Non-crystalline Solids*, vol. 483, no. 1, pp. 43–49, 2018.

[9] G. Lakshminarayana, K. A. Bashar, S. O. Baki et al., "Er3+/Dy3+ codoped B2O3-TeO2-PbO-ZnO-Li2O-Na2O glasses: optical absorption and fluorescence features study for visible and near-infrared fiber laser applications," *Journal of Non-Crystalline Solids*, vol. 503-504, no. 15, pp. 366–381, 2019.

[10] K. M. Kaky, M. I. Sayyed, A. A. Ati et al., "Germanate oxide impacts on the optical and gamma radiation shielding properties of TeO2-ZnO-Li2O glass system," *Journal of Non-crystalline Solids*, vol. 546, no. 15, Article ID 120272, 2020.

[11] V. Uma, K. Marimuthu, and G. Muralidharan, "Effect of ZnO on the spectroscopic properties of Dy3+ doped zinc telluroborate glasses for white light generation," *Journal of Non-crystalline Solids*, vol. 498, no. 15, pp. 386–394, 2018.

[12] A. Nishara Begum, V. Rajendran, "Structure investigation of TeO_2–BaO glass employing ultrasonic study," *Optical Materials*, vol. 61, no. 11-12, pp. 2143–2147, 2007.

[13] M. H. A. Mhareb, Y. S. M. Alajerami, N. Dwaikat et al., "Investigation of photon, neutron and proton shielding features of H3BO3-ZnO-Na2O-BaO glass system," *Nuclear Engineering and Technology*, vol. 53, no. 3, pp. 949–959, 2021.

[14] G. Wang, S. Xu, S. Dai, J. Yang, L. Hu, and Z. Jiang, "Thermal stability, spectra and laser properties of Yb: lead-zinc-telluride oxide glasses," *Journal of Non-Crystalline Solids*, vol. 336, no. 2, pp. 102–106, 2004.

[15] S. H. Alazouml, H. A. A. Side, M. K. Halimah, K. A. Mator, M. H. M. Zaid, and A. A. Abdulbaset, "Synthesis and elastic properties of ternary ZnO-PbO-TeO2 Glasses," *Chalcogenide Letters*, vol. 14, no. 8, pp. 302–320, 2017.

[16] K. A. Bashar, G. Lakshminarayana, S. O. Baki et al., "–––Na2O glasses," *Optical Materials*, vol. 88, pp. 558–569, 2019.

[17] N. Gupta, A. Khanna, Hirdesh, A.-C. Dippel, and O. Gutowski, "Structure of bismuth tellurite and bismuth niobium tellurite glasses and Bi2Te4O11 anti-glass by high energy X-ray diffraction," *RSC Advances*, vol. 10, no. 22, pp. 13237–13251, 2020.

[18] A. Dwivedi, C. Joshi, and S. B. Rai, "Effect of heat treatment on structural, thermal and optical properties of Eu3+ doped

tellurite glass: formation of glass-ceramic and ceramics," *Optical Materials*, vol. 45, pp. 202–208, 2015.

[19] A. Madhu, B. Eraiah, P. Manasa, and N. Srinatha, "Nd3+-doped lanthanum lead boro-tellurite glass for lasing and amplification applications," *Optical Materials*, vol. 75, pp. 357–366, 2018.

[20] N. Elkhoshkhany, E. Syala, and E. Sayed Yousef, "Concentration dependence of the elastic moduli, thermal properties, and non-isothermal kinetic parameters of Yb3+ doped multicomponent tellurite glass system," *Results in Physics*, vol. 16, Article ID 102876, 2020.

[21] U. Hoppe, E. Yousef, C. Rüssel, J. Neuefeind, and A. C. Hannon, "Structure of zinc and niobium tellurite glasses by neutron and x-ray diffraction," *Journal of Physics: Condensed Matter*, vol. 16, no. 9, pp. 1645–1663, 2004.

[22] H. N. Ritland, "Relation between refractive index and density of a glass at constant temperature," *Journal of the American Ceramic Society, Online Proofing System*, vol. 38, no. 2, pp. 86–88, 1955.

[23] K. Takayuki, "Electronic ion polarizability, optical basicity and metal (or nonmetal) binding energy of simple oxides," *Journal of the Optical Society of America B*, vol. 107, no. 1250, pp. 879–886, 1999.

[24] Y. Wang, S. Dai, F. Chen, T. Xu, and Q. Nie, "Physical properties and optical band gap of new tellurite glasses within the TeO2-Nb2O5-Bi2O3 system," *Materials Chemistry and Physics*, vol. 113, no. 1, pp. 407–411, 2009.

[25] V. Dimitrov and S. Sakka, "Linear and nonlinear optical properties of simple oxides. II," *Journal of Applied Physics*, vol. 79, no. 3, pp. 1741–1745, 1996.

[26] H. Nasu, T. Ito, H. Hase, J. Matsuoka, and K. Kamiya, "Third-order optical non-linearity of Bi2O3-based glasses," *Journal of Non-Crystalline Solids*, vol. 204, no. 1, pp. 78–82, 1996.

[27] K. Gallo and G. Assanto, "Thermal, optical and structural properties of glasses within the TeO_2-TiO_2-ZnO system," *Journal of Alloys and Compounds*, vol. 622, no. 15, pp. 333–340, 2015.